to a calibration curve for the particular crystal used) will be proportional[3] to $|E_\theta r|$.

Conclusions

Need for a knowledge of the distortion in the far-zone field pattern, as introduced by the unbalance of branch currents, is widely recognized. At the extremely short wavelengths, current symmetry is a condition obtained only with great effort and patience.

It is shown here that branch-current inequality affects the magnitude of the distant field strength for all lengths of transmitting antenna, and that, for half-lengths greater than a quarter wavelength, the shape of the field pattern also is appreciably altered.

Note that the case of $h=\lambda$, $k=0$ does not correspond to the case of $h=\lambda/2$, $k=1$. This is so because, for the former case, current distribution in the active branch is a true sine curve over an angle of 2π, while in the latter case the currents in each branch have the same sign.

For the experimental data, care was taken to detune the antenna feeders according to the method described in another paper.[4] Despite this, inequality of branch currents is apparent. An accurate measurement of the parameter k was not practicable for the data plotted in Fig. 10. Therefore, these curves may not be compared directly with the calculated curves.

Acknowledgment

The material of this paper constitutes a portion of the graduate research work performed by the author under the supervision of Professor Ronold W. P. King, of Harvard University. Indebtedness is also acknowledged to earlier material on the subject of antenna theory, completed by Dr. King, and presented by him in published papers and in lectures.

[3] Ronold King and Charles W. Harrison, Jr., "The receiving antenna," Proc. I.R.E., vol. 32, pp. 18–34; January, 1944.

[4] Ronold King, "Coupled antennas and transmission lines," Proc. I.R.E., vol. 31, pp. 638–640; November, 1943.

The Effect of Grid-Support Wires on Focusing Cathode Emission*

CHAI YEH†

Summary—**In an earlier paper, Thompson[1] has shown experimentally that sharp electron beams can be obtained if the relative electrode potentials on the anode and the grid of a vacuum tube are properly adjusted. However, theoretical interpretation of this effect was lacking. In the present paper the effects of the grid-support wires and of the various tube dimensions on the angle of electron emission are investigated theoretically. The investigation indicates that Thompson's interpretations are in the right direction. Quantitative check with the experimental results cannot be expected, because the theoretical computations are based upon pure electrostatic considerations at the cathode surface, while in actual experiments the angle of beam current at the anode is measured. Thus, the focusing and defocusing effects of the field distribution in space and the space charge existing near the cathode will cause a wide deviation between the angle of electron emission at the cathode and that of the beam current at the anode.**

I. Theory

THE PRESENT analysis makes use of a special tube. It consists of a cylindrical cathode of radius r_c and a coaxial cylindrical anode of radius r_p. Between these two cylinders, two grid wires, each of radius R, are placed on diametrically opposite sides of the cathode and at a distance r_g from it (see Fig. 1(a)). This arrangement resembles somewhat the practical construction of a beam tube with the screen grid, the beam-forming plates, and the spiral grid wires dismounted. The only portions of the grid structure remaining are the two grid-support wires. It is intended to demonstrate the importance of the contribution of these grid-support wires to the formation of an electron beam in beam tubes.

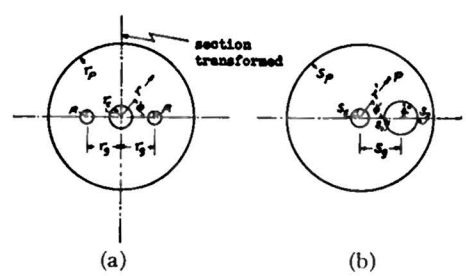

Fig. 1—Original and transformed cross section of the special tube under investigation.

It is also assumed that the effect of space charge is negligible, so that the problem is studied from a pure electrostatic point of view. In a complicated two-dimensional electrostatic problem of this type we usually make use of the "conformal transformation." In this transformation, the actual co-ordinate system is transformed into an equivalent one which makes the analysis of apparently complicated electric fields easily determinable by comparing with familiar geometry. If x and y are the co-ordinates of the original field which satisfy the two-dimensional differential equation $\partial^2 V/\partial x^2$

* Decimal classification: R138.312. Original manuscript received by the Institute, May 31, 1945; revised manuscript received, February 13, 1946.

† Radio Research Institute, National Tsing Hua University, Kunming, China.

[1] H. C. Thompson, "Electron beams and their applications in low-voltage devices," Proc. I.R.E., vol. 24, pp. 1276–1298; October, 1936.

$+\partial^2 V/\partial y^2=0$, this field can be transformed into a new system having x' and y' as co-ordinates and satisfying a similar differential equation $\partial^2 V/\partial x'^2+\partial^2 V/\partial y'^2=0$. This is to say that the Laplacian equation must be satisfied in both the actual and equivalent systems for a space-charge-free condition. The potential difference between electrodes, the capacitances, and the total charges of the original system are carried over to the new system without change, while the potential gradient and charge density may have been modified to a considerable extent.

Let us now transform half of the original section of the tube shown in Fig. 1(a) into a whole section, using the transformation

$$Z' = f(Z) \tag{1}$$

where $Z'=r'e^{j\phi'}$, $z=re^{j\phi}$. For two grid wires, the transformation formulas are

$$Z' = (Z/r_g)^2 \quad \text{or} \quad \begin{matrix} \phi' = 2\phi \\ \ln r' = 2 \ln (r/r_g). \end{matrix} \tag{2}$$

The r_g that appears in the denominator of the above equation is introduced to make the grid distance the unit of measurement for the tube dimensions. The transformed or Z'-plane view is shown in Fig. 1(b), with the following new dimensions:

The cathode radius $S_c=(r_c/r_g)^2$. The plate radius $S_p=(r_p/r_g)^2$. The inner and outer extremes of the grid wire occur at $S_1=(1-R/r_g)^2$ and $S_2=(1+R/r_g)^2$, respectively. The grid radius $R'=S_2-S_1/2$ and its distance away from the center of cathode $S_g=1/2(S_1+S_2)$. (3)

It is seen that, after transformation, the cathode radius is reduced, while the grid-wire and the anode radii are both expanded. From a pure electrostatic point of view, we may calculate the potential at any point $P(r', \phi')$ in space within the anode cylinder by considering the charges on grid, cathode, and anode, respectively. (See Fig. 2.) Let $-\lambda_1$ be the line charge located at the center

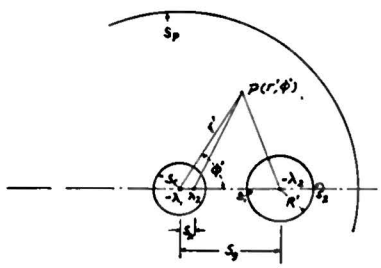

Fig. 2—Location of charges for the evaluation of the space potential at $P(r', \phi')$.

of the cathode due to charges on the anode and $-\lambda_2$ be that of the grid located at its center. Then the total charge on cathode cylinder is $-\lambda_1+\lambda_2$, where λ_2 is the image of $-\lambda_2$ on the cathode in order to make the latter an equipotential surface. The location s_k of the image charge λ_2 satisfies the equation $s_k s_g=s_c^2$.

The potential in space is then given by

$$V = \lambda_1 \ln r'^2 - \lambda_2 \ln (r'^2 + s_k^2 - 2r's_k \cos\phi') + \lambda_2 \ln (r'^2 + s_g^2 - 2r's_g \cos\phi') + c. \tag{4}$$

Equation (4) must satisfy the proper boundary conditions on the anode, the grid, and the cathode, respectively. Thus, at the anode, the proper boundary conditions are $r'=s_p$, $V=V_p$; at the cathode, they are $r'=s_c$, $V=V_c$; and using the approximations $s_p^2 \gg s_g^2$, and $s_p^2 \gg s_c^2$, (4) becomes

$$V_p - V_c = \lambda_1 \ln (s_p/s_c)^2 - \lambda_2 \ln (s_g/s_c)^2 = 2K_1\lambda_1 - 2K_p\lambda_2 \tag{5}$$

where

$$K_1 = \ln s_p/s_c \tag{6}$$

and

$$K_p = \ln s_g/s_c. \tag{7}$$

The grid surface is now no more an equipotential one. But if R is small, we may calculate the effect of the grid potential on the cathode by taking the potential at some point on the grid surface, say at a point $\phi'=0$, $s=s_2=(1+R/r_g)^2$. Then

$$V_g - V_c = \lambda_1 \ln \left(\frac{s_2}{s_c}\right)^2 - \lambda_2 \ln \frac{(s_g/s_c)^2 s_2^2 + s_c^2 - 2s_g s_2 \cos\phi'}{s_2^2 + s_g^2 - 2s_g s_2 \cos\phi'} = 2K_2\lambda_1 - 2K_g\lambda_2 \tag{8}$$

where

$$K_2 = \ln (s_2/s_c) \tag{9}$$

and

$$K_g = \ln (s_g s_2 - s_c^2)/s_c R'. \tag{10}$$

From (5) and (8), we obtain the ratio of the charges

$$\lambda_2/\lambda_1 = (K_2\alpha - K_1)/(K_g\alpha - K_p) \tag{11}$$

where

$$\alpha = (V_p - V_c)/(V_g - V_c).$$

It is assumed that on the cathode surface, if the initial velocity of the electrons is negligible, the emitted electrons are able to get out of the surface only when the field at the surface is positive. That is to say, if the field at the cathode is zero, emission is cut off. The cutoff field at cathode is found by differentiating (4) with respect to r' and letting $r'=s_c$; then

$$\left(\frac{\partial V}{\partial r'}\right)_{sc} = 2\lambda_1/s_c - 2\lambda_2/s_c \cdot \frac{s_g^2 - s_c^2}{s_c^2 + s_g^2 - 2s_c s_g \cos\phi_0'} = 0. \tag{12}$$

Solve for $\cos\phi_0'$, the cosine of the cutoff angle ϕ_0'; thus

$$\cos\phi_0' = \left[(s_c^2 + s_g^2) - \frac{\lambda_2}{\lambda_1}(s_g^2 - s_c^2)\right] \Big/ 2s_c s_g \tag{13}$$

or the cutoff angle is

$$\phi_0' = \cos^{-1}\frac{1}{2}\left[\left(\frac{s_c}{s_g}+\frac{s_g}{s_c}\right)-\frac{\lambda_2}{\lambda_1}\left(\frac{s_g}{s_c}-\frac{s_c}{s_c}\right)\right] \quad (14)$$

and the angle of electron emission is

$$\phi_e = 180 - \phi_0'. \quad (15)$$

II. Interpretations of the Theoretical Equations

From (14) and (15) it is seen that, for a definite tube structure, all the terms except α are constant, while α can be varied by adjusting the electrode potentials. Therefrom, we may deduce the following simple principles which may serve as a valuable basis for the design of beam devices:

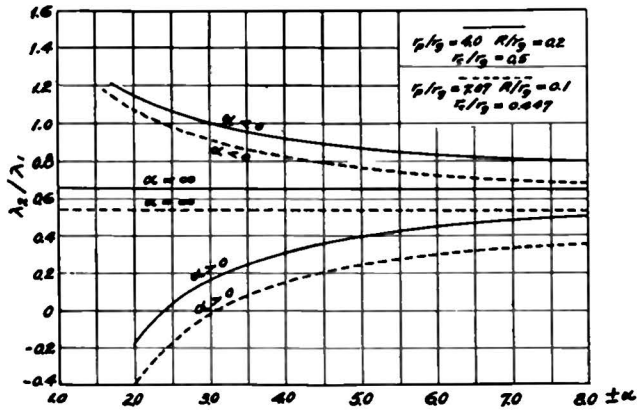

Fig. 3—Examples of the calculated ratio of charges λ_2/λ_1 for various values of $\pm\alpha$.

(1) If α, the ratio of anode to grid potentials, is kept constant, the angle of emission will be substantially constant. This is in agreement with the mathematical generalization on electron paths where initial electron

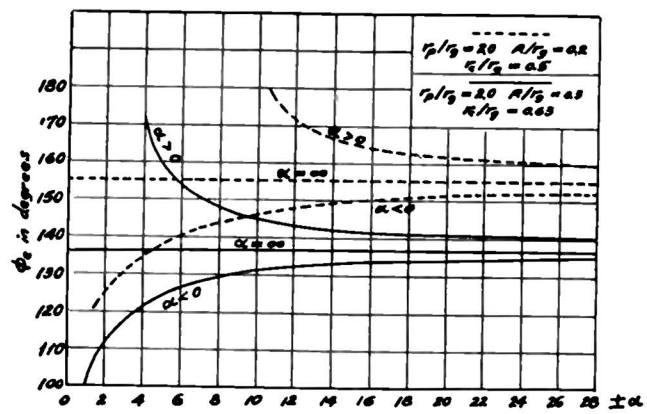

Fig. 4—Examples of the calculated angle of electron emission at cathode surface.

velocities are zero, as expressed by Langmuir and Compton.[2] Thompson's experiment indicated that for $\alpha=-3$ the beam angle measured at different anode currents is practically constant.

(2) If the grid potential is zero, then $\alpha=\infty$. Equations (14) and (15) give a constant value of emission angle for various values of the anode potentials, or

$$(\phi_e)_{\alpha=\infty} = 180 - \cos^{-1}\frac{1}{2}\left[\left(\frac{s_c}{s_g}-\frac{s_g}{s_c}\right)-\frac{K_2}{K_g}\left(\frac{s_g}{s_c}-\frac{s_c}{s_g}\right)\right] = \text{constant}. \quad (16)$$

This interpretation is also in agreement with Thompson's experiment. (See Fig. 6 of his original paper.[1])

(3) For negative values of the grid potential, i.e., $\alpha<0$, it is seen from (11) or the plot on Fig. 3 that

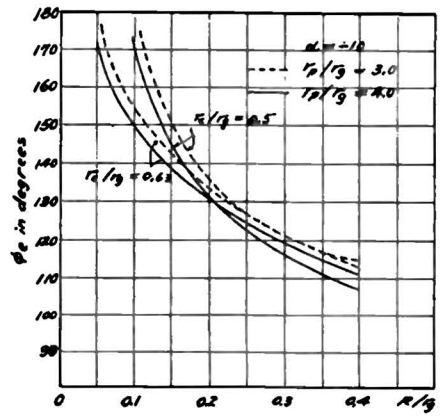

Fig. 5—Effect of varying R/r_g and r_p/r_g upon the angle of electron emission at cathode surface for $\alpha=-10$.

λ_2/λ_1 is always positive. And as the anode potential increases, keeping the grid potential unchanged, λ_2/λ_1 decreases slowly with it. Then from (14) and (15), the emission angle should increase with increasing anode potential.

For positive values of the grid potential, i.e., $\alpha>0$, it is seen that from the plot, λ_2/λ_1 increases slowly with increasing α; the emission angle is expected to decrease with it.

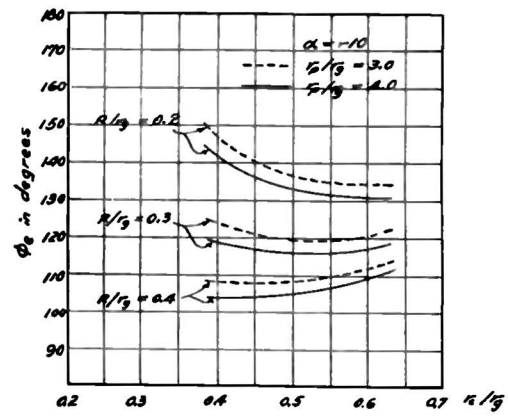

Fig. 6—Effect of varying r_c/r_g and r_p/r_g upon the angle of electron emission at cathode surface for $\alpha=-10$.

By the use of (14) and (15), the angles of emission for specific tube dimensions, at various anode-to-grid potential ratios, are calculated and plotted on Fig. 4. The upper and lower curves stand for the positive and negative potentials, respectively. The middle curve is for zero grid potential. Due to lack of data it is not possible

[2] I. Langmuir and K. T. Compton, "Electrical discharges in gases—Part II," *Rev. Mod. Phys.*, vol. 3; April, 1931.

to make a quantitative check with Thompson's results, but qualitatively they agree with each other. The theoretical results and the experimental data can not be expected to give a better check. This is because of the fact that the angle of electron emission calculated from the theoretical formulas is based upon zero off-cathode field, while in practice it is hardly possible to measure the angle of emission right at the cathode surface. What Thompson observes on the fluorescent screen is the angle of current arriving at the anode. The latter will be modified considerably by the field distribution between the electrodes. Thus, if the grid potential is negative, the equipotential lines in the neighborhood of the grid and cathode surface are of such distribution and shape as to cause the electrons to converge toward the anode. The observed angle of emission (the beam angle), therefore, will be much smaller than that calculated. If the grid potential is positive, the reverse is true.

III. The Effects of Varying Tube Dimensions

The various factors involved in the equations determining the angles of electron emission are the anode radius r_p, the grid radius R, the cathode radius r_c, and the distance r_g between centers of the grid wire and the cathode. For the tube dimensions expressed in terms of r_g, the number of variables are reduced to three. The ratio R/r_g may be interpreted either as varying R with constant r_g or varying r_g with constant R. The same is true for r_c/r_g and r_p/r_g. To find the effect of the tube dimensions on the angle of electron emission, it is first necessary to calculate the constants K_1, K_2, K_p, and K_g in (5) and (8) for various values of r_c/r_g, r_p/r_g, and R/r_g, respectively. With values of these constants, the corresponding values of λ_2/λ_1 are evaluated, and thus the angle of electron emission is calculated. Figs. 5 and 6 show the effect of these variations.

In Fig. 5, it is seen that, for smaller grid radius or larger r_g, i.e., for smaller R/r_g ratio, the effect of the grid potential is small. The angle of emission is practically determined by the anode potential and thus gives nearly complete emission from the periphery of the cathode surface. The effect of the grid potential becomes increasingly important for larger grid radius and smaller r_g, and the angle of electron emission decreases rapidly (for negative grid potentials) with increasing ratio R/r_g. The two solid-line curves are calculated for two different cathode ratios r_c/r_g, using the same r_p/r_g. The dotted-line curves are for the respective cathode ratio while using a different r_p/r_g ratio. It is seen that changing the anode ratio r_p/r_g from three to four affects the angle of emission only slightly. (See Fig. 5.)

The effect of the cathode radius on the angle of electron emission is shown in Fig. 6. If the cathode radius is small, and when it is used in combination with small R/r_g ratio, the effect of the grid potential is very small. The angle of electron emission is seen to be large. But if the cathode surface is too large, it is exposed to the influence of the anode potential to a larger extent than that of the grid potential; thus the angle of electron emission will increase with increasing cathode surface. Somewhere between these values the influence of the grid potential reaches a maximum, and the angle of electron emission is smallest (for $-\alpha$). The effect of varying r_p/r_g is also shown as dotted-line curves in this figure. Here, again, its effect on the angle of emission is rather small.

Theory and Application of Parallel-T Resistance-Capacitance Frequency-Selective Networks*

LEONARD STANTON†

Summary—**This paper deals with the theory and application of the parallel-T resistance-capacitance network, and gives a more general treatment of this network than that found in earlier papers. Using wye-delta conversion methods, the parallel-T resistance-capacitance network is represented by a single equivalent pi circuit. By introducing symbols corresponding to frequency and component values, simple expressions are derived for the impedance of the pi arms, as well as the network transmission, at any frequency. Since no arbitrary relationships are assumed between component values, the derived expressions are general.**

The practical application of the network is also considered. Three versatile circuit embodiments are described, and the effects of deviating from specified component values investigated. A calculation is made to illustrate the application of the network to a negative-feedback circuit using a single stage of voltage amplification.

* Decimal classification: R143. Original manuscript received by the Institute, July 6, 1945; revised manuscript received, January 16, 1946.

† Brown Instrument Company, Philadelphia, Pa.

Introduction

FREQUENCY-SELECTIVE networks comprising inductance and capacitance elements have been extensively discussed in the literature, and an impressive list of references is available on their theory and application. However, networks comprising resistance and capacitance elements have received less consideration, while parallel-T resistance-capacitance circuits are described, to the author's knowledge, in only two papers, by Tuttle[1] and Scott.[2] Tuttle discusses the resonant conditions of bridged-T and parallel-T

[1] W. N. Tuttle, "Bridged-T and parallel-T null circuits for measurements at radio frequencies," Proc. I.R.E., vol. 28, pp. 23–29; January, 1940.

[2] H. H. Scott, "A new type of selective circuit and some applications," Proc. I.R.E., vol. 26, pp. 226–235; February, 1938.